Magnetic properties of nanostructured ferrimagnetic zinc ferrite

C N Chinnasamy†, A Narayanasamy†, N Ponpandian†, K Chattopadhyay‡, H Guérault§ and J-M Greneche§‖

† Materials Science Centre, Department of Nuclear Physics, University of Madras, Guindy Campus, Madras 600 025, India
‡ Department of Metallurgy, Indian Institute of Science, Bangalore 560 012, India
§ Laboratoire de Physique de l'Etat Condensé, UPRESA CNRS 6087, Université du Maine, Faculté des Sciences, 72085 Le Mans Cedex 9, France

E-mail: greneche@univ-lemans.fr

Abstract. Nanostructured $ZnFe_2O_4$ ferrites with different grain sizes were prepared by high energy ball milling for various milling times. Both the average grain size and the root mean square strain were estimated from the x-ray diffraction line broadening. The lattice parameter initially decreases slightly with milling and it increases with further milling. The magnetization is found to increase as the grain size decreases and its large value is attributed to the cation inversion associated with grain size reduction. The ^{57}Fe Mössbauer spectra were recorded at 300 K and 77 K for the samples with grain sizes of 22 and 11 nm. There is no evidence for the presence of the Fe^{2+} charge state. At 77 K the Mössbauer spectra consist of a magnetically ordered component along with a doublet due to the superparamagnetic behaviour of small crystalline grains with the superparamagnetic component decreasing with grain size reduction. At 4.2 K the sample with 11 nm grain size displays a magnetically blocked state as revealed by the Mössbauer spectrum. The Mössbauer spectrum of this sample recorded at 10 K in an external magnetic field of 6 T applied parallel to the direction of gamma rays clearly shows ferrimagnetic ordering of the sample. Also, the sample exhibits spin canting with a large canting angle, maybe due to a spin-glass-like surface layer or grain boundary anisotropies in the material.

1. Introduction

Small particles of magnetic materials exhibit interesting magnetic properties [1, 2]. Recently fine particles of spinel ferrites synthesized by sol–gel or mechanochemical methods were shown to have magnetic properties markedly different from that of their bulk counterparts. Of all the spinel systems, $ZnFe_2O_4$ is found to be the most interesting one to study the effect of grain size on the magnetic properties. $ZnFe_2O_4$ is a normal spinel in the crystalline bulk form with Zn^{2+} ions only on the A-sites and Fe^{3+} ions only on the B-sites and is characterized as an ordered antiferromagnet below 10 K. Any change in the cation distribution in this ferrite due to grain size reduction, therefore, can easily be studied. In view of this a considerable amount of research has been done to investigate the effect of grain size on the cation distribution and magnetic properties of nanocrystalline $ZnFe_2O_4$ [3–10]. All these studies agree in one aspect that $ZnFe_2O_4$ is magnetically ordered with high ordering temperature and magnetic moment. But they differ in predicting the type of magnetic ordering. Some of them conclude

‖ Author to whom all correspondence should be addressed.

that nanocrystalline $ZnFe_2O_4$ is ferromagnetically ordered due to clustering of Fe^{3+} ions and only one report published very recently predicts that the magnetic ordering is of ferrimagnetic type in the case where zinc ferrite ultrafine powders were prepared by the supercritical sol–gel method [11]. Goya *et al* [12] have synthesized nanocrystalline $ZnFe_2O_4$ by using the mechanochemical method. The main conclusions from their study are (i) the presence of competing ferro- and antiferromagnetic exchange interactions arising from Fe clustering, (ii) the breaking of superexchange bonds due to oxygen vacancies produced while milling and (iii) the decrease of hyperfine magnetic fields with milling process due to oxygen vacancies. Also, magnetization does not saturate even under a magnetic field of 6.5 T. The Mössbauer isomer shifts show evidence for the presence of the Fe^{2+} charge state formed due to the oxygen vacancies. Jiang *et al* [13] have produced nanocrystalline $ZnFe_2O_4$ by ball milling the bulk ferrite prepared by using the conventional ceramic route. From the increase in the relative intensities of the second and fifth lines of the Mössbauer sextet in a small external magnetic field of 0.7 T applied perpendicular to the gamma ray direction, they conclude that the magnetic ordering could be either ferromagnetic or ferrimagnetic.

In order to confirm the type of magnetic ordering and to study the effect of grain boundary and surface spins on the magnetic properties of nanostructured $ZnFe_2O_4$, we have carried out Mössbauer and magnetization studies on different nanostructured powders of $ZnFe_2O_4$. They were prepared by high energy mechanical milling from the crystalline bulk $ZnFe_2O_4$ obtained by the conventional ceramic route. It is important to remember that, in the synthesis of nanostructured particles using mechanical milling, nanocrystalline grains are welded to each other through grain boundaries. Our results confirm without any ambiguity that milled $ZnFe_2O_4$ powders exhibit ferrimagnetic ordering due to change in the cation distribution when the grain size is reduced to the nanometre scale. The system also shows spin canting due to a spin-glass-like surface layer or grain boundary anisotropies in the material.

2. Experiment

Zinc ferrite was synthesized in polycrystalline form by the conventional ceramic method from a mixture of α-Fe_2O_3 (Cerac, 99.95%) and ZnO (Cerac, 99.5%) taken in the atomic ratio of 1:1 respectively. The formation of single-phase spinel was confirmed by x-ray powder diffraction using Fe Kα ($\lambda = 1.9373$ Å) radiation and a long time pattern using Cu Kα ($\lambda = 1.54056$ Å) radiation to obtain a structural and a microstructural insight into the nanostructured powders milled for 20 h. The milling of the as-prepared $ZnFe_2O_4$ was carried out in air in a planetary ball mill (Fritsch Pulverisette, P7) with tungsten carbide balls and vials to reduce the grain size. After selected milling times, a small amount of powder was removed from the vial for analysis. The chemical analysis of these samples confirmed that they have very low levels of impurity elements (a small amount of WC estimated at about 5 wt% resulting from the balls and vials).

Magnetic measurements were carried out at the University of Madras, India using a vibrating sample magnetometer (EG&G PARC, model 4500) with a maximum available field of 7 kOe. ^{57}Fe Mössbauer spectrometry was carried out at Le Mans, France at different temperatures with and without external magnetic field using a constant acceleration Mössbauer spectrometer with a source of 25 mCi ^{57}Co diffused into an Rh matrix. Natural iron foil was used as a standard for velocity calibration.

3. Results and discussion

3.1. X-ray studies

The x-ray diffractograms of the as-prepared (0 hour) and the milled samples for various milling times are shown in figure 1. The milled zinc ferrite samples retain their spinel structure
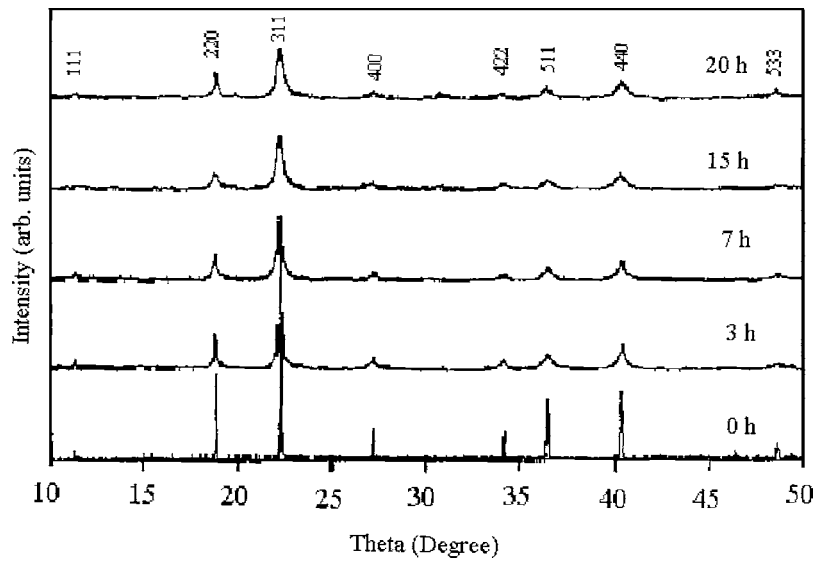
Figure 1. X-ray diffractograms (Fe Kα) of ZnFe$_2$O$_4$ milled for various times.
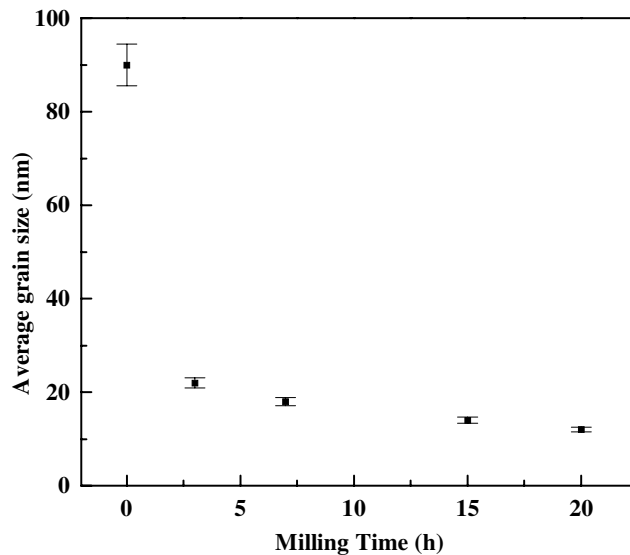

Figure 2. Average grain size of ZnFe$_2$O$_4$ powders versus milling time.

(Frankilinite, JCPDS 22-1012). The average grain size and root mean square (rms) atomic-level strain $\langle \varepsilon^2 \rangle^{1/2}$, were estimated from the diffraction line broadening. The x-ray line broadening increases with milling time due to the reduction of grain size and increase in the atomic level strain. The average grain size was determined by using the Scherrer formula from the full width at half maximum of the (311) diffraction line and is shown in figure 2 for different milling times. The grain size decreases with milling time and reaches 11 nm for the 20 hours milled sample. The rms strain increases with milling and becomes constant after 15 hours of milling as seen from figure 3. The lattice parameter initially decreases slightly with milling
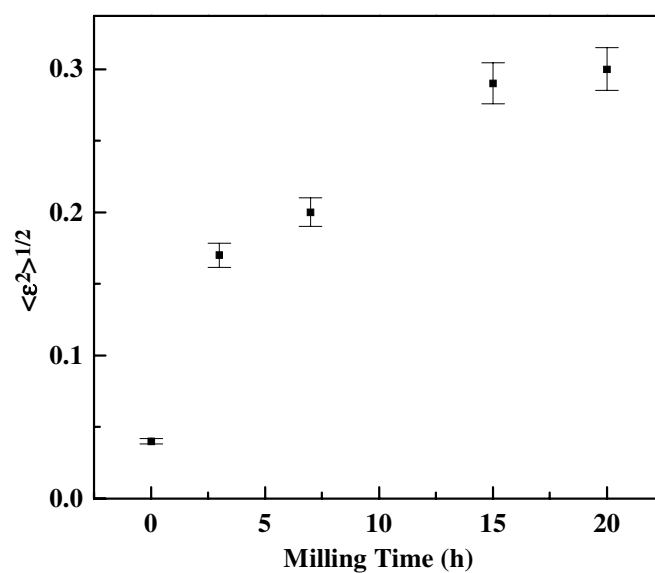
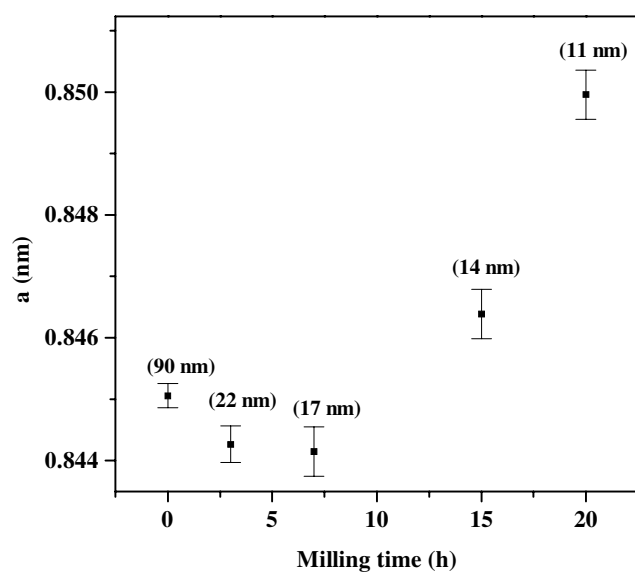**Figure 3.** The root mean square strain versus milling time.

Figure 4. Lattice parameter versus milling time for nanocrystalline $ZnFe_2O_4$.

and it increases for larger durations of milling as seen from figure 4. The increase in the lattice parameter after 7 hours of milling may be due to the redistribution of cations from normal spinel structure. An x-ray diffraction pattern of the 20 hours milled sample was collected on a Philips diffractometer with Cu Kα radiation in the range of $2\theta = 15$ to $120°$ in steps of $0.02°$. In this case, the structural and microstructural parameters were refined using the Rietquan procedure which is well adapted for broadened diffraction peaks and based on the Rietveld method combined with a Fourier analysis [14]. The refined values well agree with
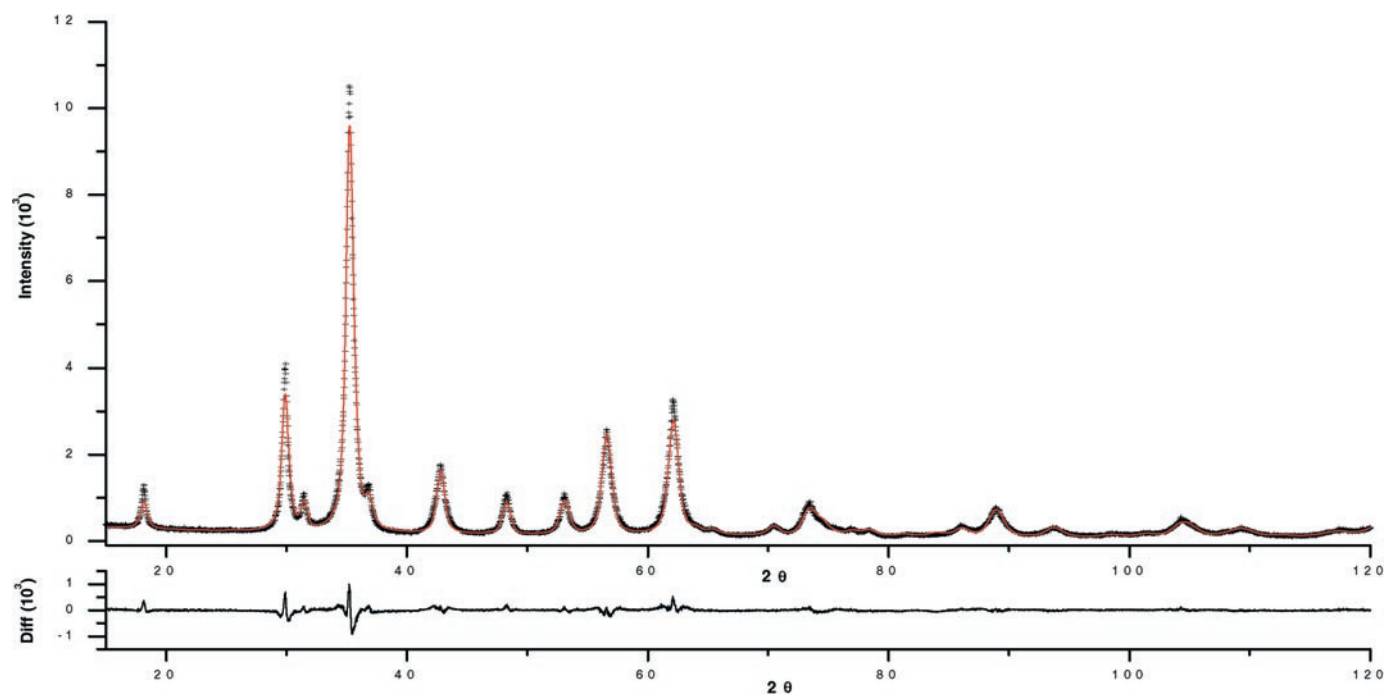
Figure 5. X-ray diffractogram (Cu Kα) of the 20 hours milled ZnFe$_2$O$_4$. The continuous curve is the result of fitting using the Rietquan procedure.
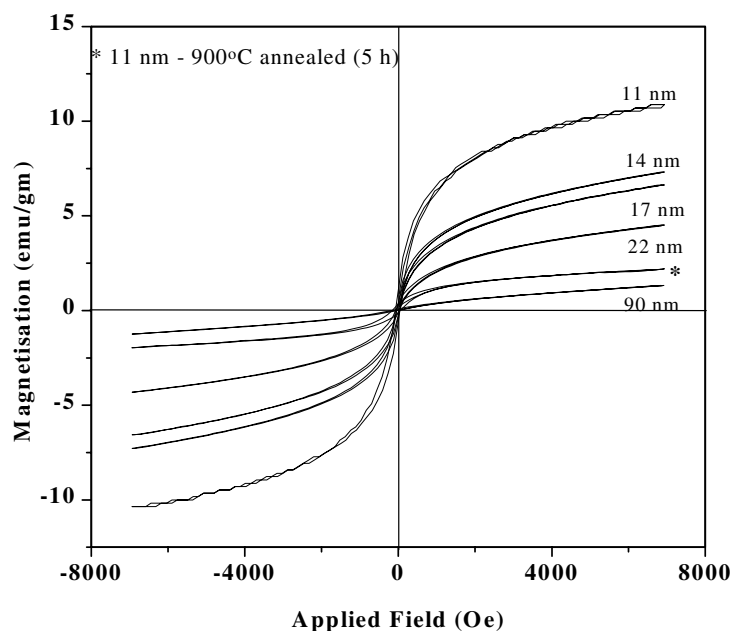
Figure 6. The $M–H$ loops of $ZnFe_2O_4$ at 300 K for different grain sizes. (*) the 11 nm sample was annealed for 5 hours at 900 °C.

that determined above using the Scherrer formula. It is important to emphasize that only a single component allows us to describe the x-ray pattern as shown in figure 5, in contrast to that of nanostructured fluoride powders where a second component assigned to the disordered grain boundaries had to be introduced [15]. One concludes that the present nanostructured $ZnFe_2O_4$ powders do not contain a significant contribution of grain boundaries (<15 at.%).

3.2. Magnetization studies

The magnetization of $ZnFe_2O_4$ was determined for different grain sizes at room temperature. Figure 6 shows that the $M–H$ loops of the as-prepared and milled samples could not be saturated with the available maximum field of 7 kOe. This is an indication of the presence of large anisotropy in the material. The magnetization increases as the grain size decreases and this can be explained by the redistribution of cations in the nanocrystalline $ZnFe_2O_4$. In bulk form, $ZnFe_2O_4$ is a normal spinel with Zn^{2+} ions located in the A-sites and Fe^{3+} ions in the B-sites; it behaves as an antiferromagnet below 10 K and a paramagnet above this temperature. The $M–H$ loops observed in the present study show that the cation distribution has changed from the normal to the mixed spinel type. Hence some percentage of Fe^{3+} ions is pushed to the tetrahedral sites which switches on the A–B super-exchange interaction between Fe^{3+} ions on both the sites and gives rise to ferrimagnetic ordering. EXAFS studies conducted by Jeyadevan *et al* [16] for the co-precipitated nanocrystalline $ZnFe_2O_4$ also support the presence of some Zn^{2+} ions on the B-site and Fe^{3+} ions on the A-site. The neutron diffraction study [17] of nanocrystalline $ZnFe_2O_4$ reports that the occupancy of Fe^{3+} ions at the A-sites is 0.018 and 0.142 for the fine particles of diameters 96 and 29 nm respectively. The unsaturated magnetization behaviour observed in nanocrystalline zinc ferrite reveals the presence of a superparamagnetic and single domain nature of the particles [18]. The sample with 11 nm
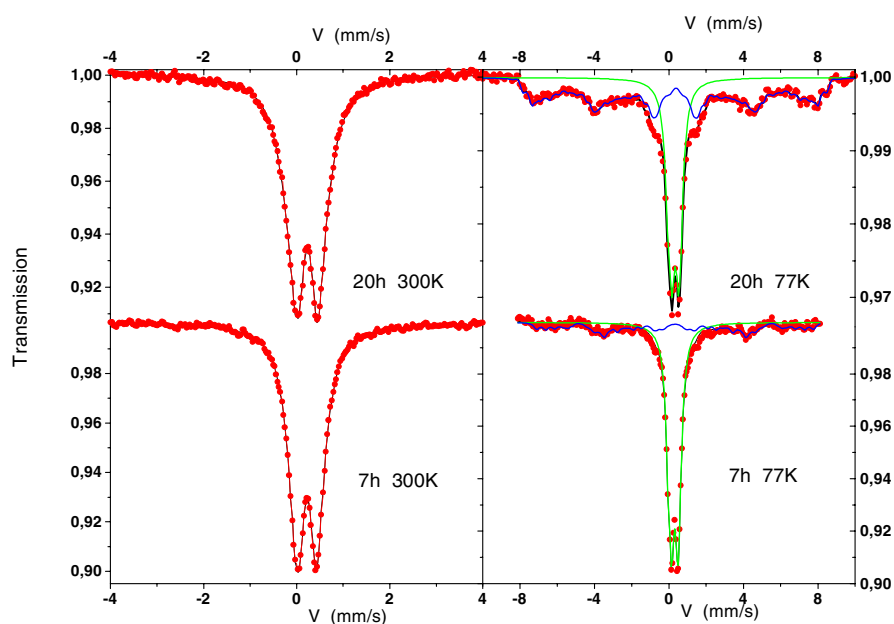
Figure 7. Mössbauer spectra recorded at 77 K and 300 K on $ZnFe_2O_4$ powders milled for 7 and 20 h corresponding to the grain sizes of 22 and 11 nm, respectively.

Table 1. Mössbauer parameter isomer shift (IS) relative to that of α-Fe at 300 K, quadrupole splitting Δ, quadrupole shift 2ε and the hyperfine magnetic field $\langle B \rangle$ of the spectra at 77 and 300 K of nanocrystalline $ZnFe_2O_4$ milled for 7 h (22 nm) and 20 h (11 nm).

Sample	T (K)	$\langle IS \rangle$ (mm s^{-1}) ± 0.01	$\langle \Delta \rangle$ (mm s^{-1}) ± 0.01	% ± 2	$\langle IS \rangle$ (mm s^{-1}) ± 0.01	$\langle 2\varepsilon \rangle$ (mm s^{-1}) ± 0.01	$\langle B \rangle$ (T) ± 1	% ± 2
7 h milled	300	0.34	0.47	100	—	—	—	0
	77	0.44	0.38	71	0.48	0.02	33	29
20 h milled	300	0.33	0.56	100	—	—	—	0
	77	0.45	0.41	39	0.48	0.01	34	61

grain size was annealed for 5 hours at 900 °C. Its magnetization decreases and exhibits a behaviour similar to that of the 90 nm samples.

3.3. Mössbauer studies

The ^{57}Fe Mössbauer spectra recorded at 300 K and 77 K for the samples with grain sizes of 22 (7 h) and 11 nm (20 h) are given in figure 7. The spectra of the two samples appear to be similar at 300 K except for a larger line width for the sample with 11 nm grain size. The spectra were least-squares fitted and the refined values of the hyperfine parameters are given in table 1. The values of isomer shift and quadrupole splitting are characteristic of Fe^{3+} charge state. There is no evidence for the presence of Fe^{2+} charge state due to oxygen vacancies produced by milling as observed by Goya and Rechenberg [12].

The Mössbauer spectra of these two samples recorded at 77 K are qualitatively similar but differ quantitatively. The main relevant hyperfine parameters are listed in table 1. The spectra

consist of a magnetically ordered component and a quadrupole doublet and the latter may be due to the superparamagnetic behaviour of small particles. For the samples with smaller grain size, the relative intensity of the magnetically ordered component is greater (61%) than that of the other sample (29%) with a larger grain size. This is a clear evidence for the increase of the cation inversion parameter with decrease of grain size.

Prolonged ball milling induces ferrimagnetic moment at 300 K as is evident from figure 6 but magnetically ordered Mössbauer spectra are obtained only from 77 K. The observed difference between the two measurements is due to the magnetic relaxations in the small grains, namely superparamagnetism and collective magnetic excitations. The magnetic field applied in the magnetization measurements greatly suppresses the relaxation leading to the measurement of non-zero magnetic moment whereas a broad quadrupolar doublet is obtained in the Mössbauer spectrum due to superparamagnetic behaviour of the sample. At low temperatures the relaxation effects are slowed down and a magnetically ordered Mössbauer spectrum is observed. Similar results have been obtained by Hamdeh *et al* [4] also.

The 4.2 K Mössbauer spectra given in figure 8 for the samples with 11 nm and 22 nm grain size show that both the powders are magnetically well ordered and the thermal fluctuations of the magnetization have completely disappeared at this temperature. The shape of the Mössbauer spectrum suggests that the Fe sites possess different atomic environments. The spectra have been well fitted with at least three sextets but fitting models involving more sextets can be also used. The relative line intensities of the sextets were constrained to a 3:2:1 ratio as the samples are randomly oriented. Consequently, the refined values of the Mössbauer parameters do not allow at this stage a clear description of the sample. Nevertheless, the values of some relevant hyperfine parameters which are listed in table 1 are consistent with those proposed by Dickof *et al* on substituted zinc spinel ferrite [19].

The Mössbauer spectrum of the 11 nm grain size powder recorded at 10 K in an external magnetic field of 6 T is shown in figure 8. The hyperfine structure reveals a splitting of outermost lines and a significant decrease of intermediate line intensities. The first fitting model consists in two magnetic components, the inner one with broad lines. The second model which is reported in figure 8 is based on three magnetic components in agreement with the zero-field model refinement. A discrete distribution of hyperfine fields has been also used, giving rise to similar results. According to the isomer shift values, the effective field and its orientation respective to the applied field, the two main components are clearly assigned to tetrahedral (low isomer shift, high effective field) and octahedral (high isomer shift and low effective field) iron sites of $ZnFe_2O_4$ crystalline grains. The values of hyperfine and effective fields, quadrupole shift and isomer shift of the various components of the Mössbauer spectra are given in table 2.

The third sextet which arises from Fe^{3+} ions in the B-sites exhibits broad lines, indicating different kinds of environment. Our earlier studies on some bulk spinel ferrites also report more than one sextet from the B-sites due to different local environments of Fe^{3+} ions [20, 21]. The non-vanishing intensity of the second and fifth lines for all the three sextets is clear evidence for Fe spin canted structures in both A- and B-sites, with respect to the applied field. The average canting angles have been calculated from the ratios of the line intensities of $A_{2,5}$ to $A_{1,6}$ and the values are given in table 2.

The following relationship:

$$\langle B \rangle^2 = \langle B_{eff} \rangle^2 + B_{app}^2 - 2B_{app}\langle B_{eff}\rangle \cos\langle\beta\rangle \tag{1}$$

allows us to estimate the hyperfine field B where B, B_{eff}, B_{app} and β correspond to the mean hyperfine field, the mean effective field (equal to the vectorial sum of the hyperfine and the applied fields), the external field and the mean angle between the directions of the effective field
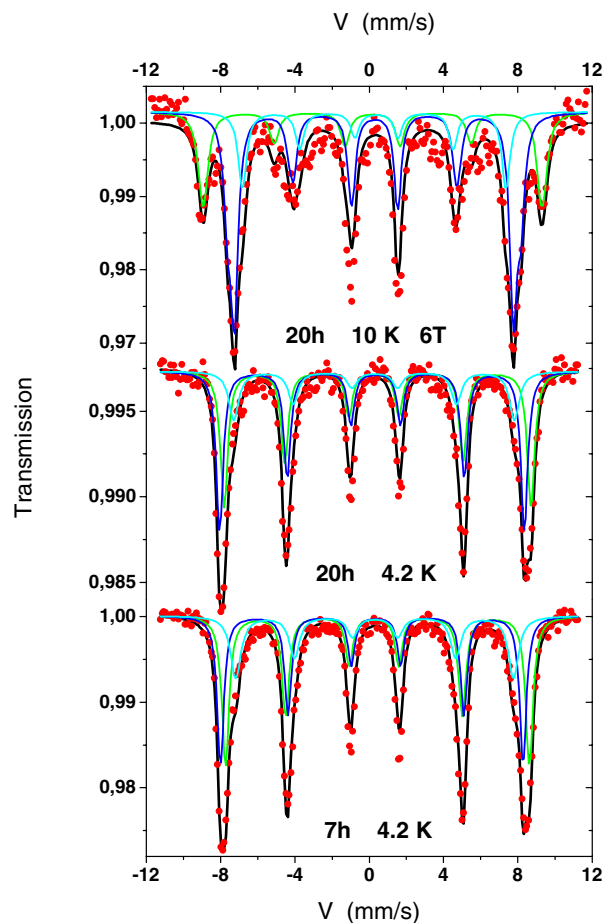
Figure 8. Zero-field Mössbauer spectra recorded at 4.2 K for the 7 and 20 hours milled $ZnFe_2O_4$ samples and 6 T in-field Mössbauer spectrum recorded at 10 K for the 20 hours milled $ZnFe_2O_4$ sample.

and the γ-beam, i.e. the applied field, respectively. The small disagreement can be explained by the fitting errors due to the strong overlap of lines of the zero-field spectrum and by the angle distributions of Fe magnetic moments. Because of the weak anisotropy, the observed large values of canting angles might have two main origins: (i) competing antiferromagnetic interactions due to the Zn–Fe disorder at A- and B-sites and (ii) a spin-glass-like surface layer or grain boundary anisotropies in the material. The third sextet with a smaller hyperfine field and a large canting angle of $45°$ can also be attributed to Fe^{3+} ions occupying the grain boundaries or surfaces with a highly disordered structure.

Oliver *et al* [11] have prepared samples by the sol–gel method and reported ferrimagnetic ordering for their samples. They could resolve the A- and B-site Mössbauer signals by applying an external magnetic field of 7 T in the direction of gamma rays. However, their finding of the presence of B–B antiferromagnetic interaction below 10 K is not understandable. Mössbauer spectra of their samples show slow relaxation process at 4.2 K and fast relaxation process at high temperatures. Our studies agree with that of Oliver *et al* [11] in one aspect that $ZnFe_2O_4$ is ferromagnetically ordered in nanocrystalline form irrespective of the method of preparation of

Table 2. Mössbauer parameters of nanocrystalline $ZnFe_2O_4$ milled for 7 and 20 h at 4.2 K in zero magnetic field and that milled for 20 h at 10 K in an external magnetic field of 6 T applied parallel to the direction of gamma rays. The data are obtained from a three six-line component fitting model (see text). Isomer shift values (IS) relative to that of α-Fe at 300 K, quadrupole shift 2ε, hyperfine field B, effective field B_{eff}, average canting angle β and relative proportions I_{rel}.

Sample	Site	IS (mm s^{-1}) ± 0.02	$\langle 2\varepsilon \rangle$ (mm s^{-1}) ± 0.02	$\langle B \rangle$ (T) ± 0.5	$\langle B_{eff} \rangle$ (T) ± 0.5	$\langle \beta \rangle$ (°) ± 5	I_{rel} (%) ± 2
7 h	B-type	0.51	0.19	50.5		—	40
4.2 K	A	0.41	−0.22	50.3			36
	B-type	0.48	0.01	46.1			24
20 h	B-type	0.51	0.20	51.0		—	38
4.2 K	A	0.41	−0.20	50.7			43
	B-type	0.49	−0.04	46.6			19
20 h	B-type	0.52	0	49.6[a]	47.1	37	58
10 K	A	0.42	0	51.5[a]	56.4	35	24
6 T	B-type	0.51	0	47.0[a]	43.7	45	18

[a] Hyperfine field estimated from B_{eff} and β.

the samples. However, the Mössbauer spectra of our samples are not affected by the relaxation process as has been observed by them. This also supports our claim that there are no Fe^{2+} ions in our samples.

Further studies are in progress to confirm whether there are two types of spin aligned in opposite directions in octahedral sites below the antiferromagnetic Néel temperature of 10 K as reported by Oliver *et al* [11] and also to determine the cation inversion parameter and spin canting as a function of grain size.

4. Conclusions

Nanostructured $ZnFe_2O_4$ powders have been prepared with different grain sizes by ball milling bulk $ZnFe_2O_4$ synthesized by the conventional ceramic route. Nanocrystalline $ZnFe_2O_4$ gives rise to a large magnetization at high temperatures with its value increasing with decrease of grain size. The ferrimagnetic ordering of nanocrystalline $ZnFe_2O_4$ is confirmed from our Mössbauer studies. The observed spin canting of ^{57}Fe spins in both the A- and B-sites may be due to the spin-glass-like surface layer or grain boundary anisotropies in the material.

References

[1] Tkacovba K, Sepelak V, Sterklora N and Noldyrev V V 1996 *J. Solid State Chem.* **123** 100
[2] Chinnasamy C N, Narayanasamy A, Ponpandian N and Chattopadhyay K 2000 *Mater. Sci. Eng.* A at press
[3] Schissel W *et al* 1996 *Phys. Rev.* B **53** 9143
[4] Hamdeh H H, Ho J C, Oliver S A, Wiley R J, Oliveri G and Busca G 1997 *J. Appl. Phys.* **81** 1851
[5] Clark Ted M and Evans B J 1997 *IEEE Trans. Magn.* **33** 3745
[6] Yokayama M, Ohta E, Sato T, Komaba T and Sato T 1997 *J. Physique Coll.* IV **7** C1 521
[7] Battle J, Clark T and Evans B J 1997 *J. Physique Coll.* IV **7** C1 257
[8] Hamdeh H H, Ho J C, Oliver S A, Wiley R J, Kramer J, Chen Y Y, Lin S H, Yao Y D, Datiro M and Busca G
       1995 *IEEE Trans. Magn.* **31** 3808
[9] Sato T, Haneda K, Seki M and Iijima T 1990 *Appl. Phys.* A **50** 13
[10] Anantharaman M R, Jagatheesan S, Malini K A, Sindhu S, Narayanasamy A, Chinnasamy C N, Jacops J P,
       Reijne S, Seshan H and Brongersma R H H 1998 *J. Magn. Magn. Mater.* **189** 83
[11] Oliver S A, Hamdeh H H and Ho J C 1999 *Phys. Rev.* B **60** 3400
[12] Goya G F and Rechenberg H R 1999 *J. Magn. Magn. Mater.* **196** 191
[13] Jiang J Z, Wynn P, Morup S, Okada T and Berry F J 1999 *Nanostruct. Mater.* **12** 737
[14] Lutterotti L and Scardi P 1990 *J. Appl. Cryst.* **23** 246
[15] Guérault H and Greneche J M 2000 *J. Phys.: Condens. Matter* **12** 4791
[16] Jeyadevan B, Tohiji K and Nakatsuka K 1994 *J. Appl. Phys.* **76** 6325
[17] Lotzering F K 1996 *J. Phys. Chem. Solids* **27** 139
[18] Bean C P and Livingston J D 1959 *J. Appl. Phys.* **30** 120S
[19] Dickof P A, Schurer P J and Morrish A H 1980 *Phys. Rev.* B **22** 115
[20] Narayanasamy A and Häggström L 1983 *J. Phys. C: Solid State Phys.* **16** 591
[21] Sundararajan M D, Narayanasamy A, Nagarajan T, Häggström L, Swamy C S and Ramanujachary K V 1984
       J. Phys. C: Solid State Phys. **17** 2953